

BEARING CAPACITY OF SMOOTH AND ROUGH SQUARE AND RECTANGULAR FOOTINGS ON CLAY

Jubayer¹, Shafiqul Islam² and Rokonzaman³

¹Student, Khulna University of Engineering & Technology, Bangladesh,
e-mail: jubayer92bayezid@gmail.com.

²Assistant Professor, Khulna University of Engineering & Technology, Bangladesh,
e-mail: sumon2k8@yahoo.com.

³Professor, Khulna University of Engineering & Technology, Bangladesh,
e-mail: rokoncekuet@yahoo.com.

ABSTRACT

The Uniaxial Vertical bearing capacity of smooth and rough square and rectangular footings resting on homogeneous undrained clay is investigated with finite element analyses. The results are compared with the conventional and available analytical and numerical solutions. Finally a best estimate of bearing capacity and shape factor are derived as a function of aspect ratio. The bearing capacity of rough square footing is 5.36% greater than the bearing capacity of smooth square footing.

Keywords: Bearing capacity, Square footings, Rectangular footings, Aspect ratio.

1. INTRODUCTION

Traditional bearing capacity theory, developed based on conditions of plane strain (Terzaghi 1943), is suitable for strip footings where the length of the footing is “long” relative to its breadth. Many shallow foundations, particularly those used off shore, have a lower aspect ratio with a rectangular or square foot print. Edge effects improve bearing capacity (per unit area) of a three-dimensional footing compared to a strip footing as slip planes must develop around the perimeter of the three dimensional footing as opposed to only adjacent to the “long” edge under conditions of plane strain.

For the bearing capacity of square and rectangular footing no exact solution exists, even for the simple case of a surface footing resting on an isotropic, homogeneous deposit obeying an undrained failure criterion. However, the bearing capacity factors and shape factors for square and rectangular footings are bracketed with respect to strip footing.

Some studies have been carried out for bearing capacity of square and rectangular footings. Shield and Drucker(1953) proposed an upper bound solution for the ultimate limit state under uniaxial vertical loading for smooth rectangular footings, which gave a bearing capacity factor for a square footing of $N_c=5.71$. Later Michalowski and Dawson(2002) proposed a lower bearing capacity factor of $N_c=5.43$ based on finite difference analyses.

Michalowski (2001) proposed an upper bound solution for a rough square footing, giving a bearing capacity factor $N_c=6.56$ which is higher than the bearing capacity factor for square and rectangular footings.

The paper presents finite element analyses for smooth and rough square footings and proposes best estimates of the bearing capacity factors for rough rectangular footings of varying aspect ratio. The kinematic failure mechanism of square and rectangular footings observed are also

presented. For a square footing the failure mechanism indicates fourfold symmetry with displacement orthogonal to the edges. But it can be said that this analyses will provide a useful starting point for a better alternative upper bound solution.

2. METHODOLOGY

All the finite element analyses were carried out using the software ABAQUS. Two dimensional model was developed for strip footing analysis and three dimensional footing was developed for both square and rectangular rough and smooth footing. For two dimensional footing and three dimensional footing meshing, materials and load path was different.

Two dimensional footing was modeled for strip footing where length is relatively long than breadth. On surface footing at first we performed element study to fix the element size and meshing as well as displacement. The fixation of mesh element size is an important part of modeling because it determines the amount of element number and time required for the analysis of the model. After fixation of the element size, the type element also selected whether it is linear, quadratic or triangular. The quadratic element shows more accurate result and load-displacement curve become constant very quickly. Although triangular element shows more accurate result compared to quadratic but to avoid time for the analysis we used quadratic element. The load applied on the footing loaded area and gravity load all over the model element. For smooth footing the displacement occurred both vertically and laterally and no lateral displacement are restrained to zero. On the other hand for rough footing lateral displacement are restrained to zero and only vertical displacement occurred. Time increment for the analysis of two dimensional model was varied with different steps.

Two dimensional footings are also checked to investigate the results changing with the width. The footing was analyzed for footing width 0.5m, 1m, 2m, and 5m and found the bearing capacity results comparing with each other. Footing was also analyzed by changing the ratio of $E_u/s_u = 100, 250, 500, 2000, 5000, 10000, 30000$ to compare the results to check whether the results vary or not.

After completed the data check then the model was submitted for the analysis. After completed the analysis of the model the failure diagram for the undeformed shape was viewed and load-displacement curve plotted with the output data. With the output data we calculated the ultimate bearing capacity (Q_u) as well as bearing capacity factor. From three dimensional model analysis for both rough and smooth square and rectangular footing the kinematic failure mechanism was compared and best fit equation was developed for footing shape factor. Although three dimensional footing analysis required more time than the two dimensional footing as the number of element was high in three dimensional compared to the two dimensional footing. If the meshing is not good enough the element becomes distorted which will hamper the results as well as affect the exactness of the best estimate equation. The more the meshing finer the more it gives smooth failure pattern as well as give more accurate result.

2.1 Mesh

The two-dimensional finite element mesh used for analysis of a strip footing of width B and Length zero considered. The mesh extended $10B$ from the edges of the footing and $10B$ beneath the footing.

A number of mesh densities were investigated to achieve a time efficient model without maintaining accuracy and mesh element type was a 4-node bilinear plane strain quadrilateral,

reduced integration and hourglass control. Meshing was done for linear, quadratic and triangular element to fix the element for the model and to determine which provide more accurate results.

Six three-dimensional models were modeled to investigate the effect of varying footing length to breadth aspect ratio on bearing capacity of $L/B=1$ (square), 2, 3, 4, 5, and 10. For the longer footings more elements were used in the longitudinal direction to maintain uniform element size across the models. For example the mesh for the $L=B$ comprises 11700 and the mesh for the $L=5B$ footing comprises 25200 linear hexahedral element (more than twice as many as the square footing mesh) shown in Figure 1.

2.2 Load Path

All the finite element analysis were carried out to investigate the ultimate load (Q_u). Ultimate load $Q_u = \sum \text{sum of vertical reaction force at all nodes } (RF_2) / \text{Footing area}$. The presence of rigid footing is modeled by applying uniform vertical downward displacements at the nodal points at the top surface. Horizontal displacement at the footing-soil interface were restrained to zero for rough footing $U_1=0$ $U_2=\text{prescribed displacement at the contact nodes}$, $U_3=0$ (for rough footing) and free for smooth footing where, $U_1 \neq 0$ $U_2=\text{prescribed displacement at the contact nodes}$, $U_3 \neq 0$.

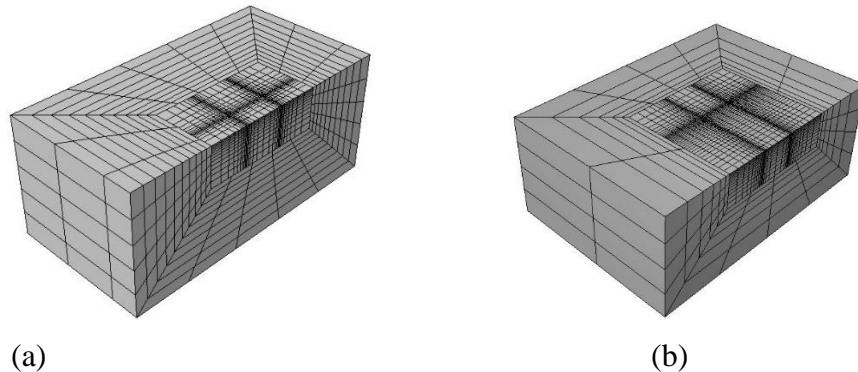


Figure 1: Finite element meshes (a) square footing ($L=B$); (b) rectangular footing ($L=5B$).

3. ILLUSTRATIONS

3.1 Comparison of bearing capacity as function of footing aspect ratio

In addition to the square footing analyses, six analyses were carried out on rectangular footings to investigate the effect of aspect ratio (Length to breadth, L/B). All the rectangular footing analyses were modeled for a rough interface on the underside of the footing.

Figure 2 represents comparison of bearing capacities as a function of aspect ratio for square and rectangular footings with a rough and smooth interface from the finite element results from this study with Skempton's empirical expression and other available bound solutions. Here, we see that the more the aspect ratio increases the more the difference between square and rectangular footing increases. That means for square footing the difference between bearing capacity of smooth and rough footing is maximum and the more the footing tends to strip footing the difference becoming lesser. The most visible thing is that the bearing capacity of rough and smooth based square and rectangular footings are lies in between the lower bound and upper bound solutions.

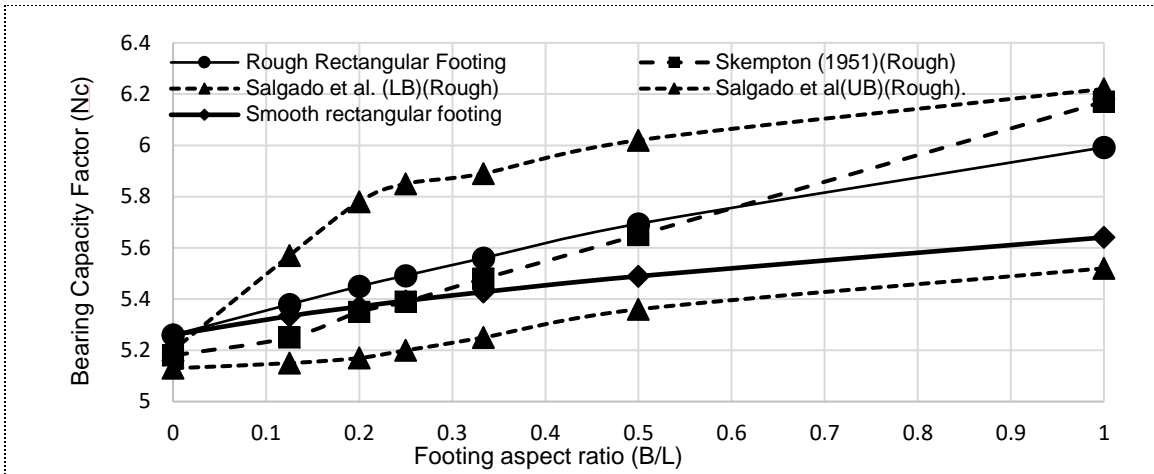


Figure 2: Comparison of Bearing Capacity Factor as function of Footing aspect ratio with available published data by Finite Element Analyses.

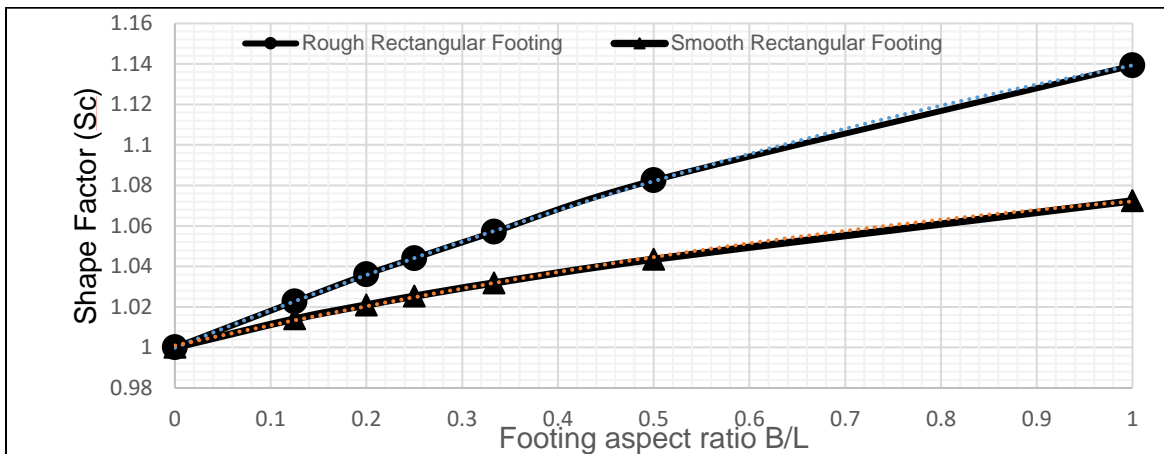
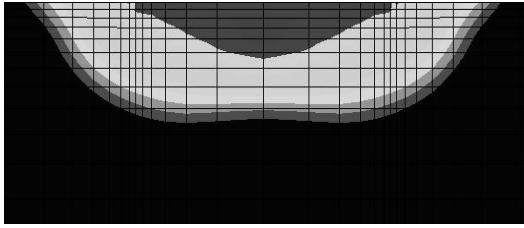


Figure 3: Best-estimate shape factors for square and rectangular footings.

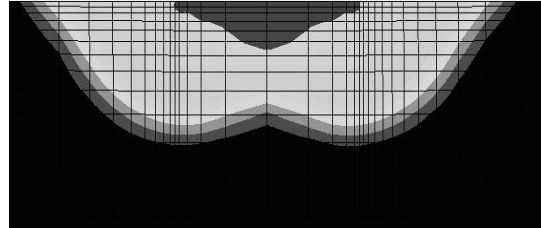
The best estimate shape factors for square and rectangular footings are obtained from the Figure 3. It is clearly visible that the difference between smooth and rough square and rectangular footings decrease with the decrease of aspect ratio. The shape factor define as the ratio of bearing capacity of rectangular footing to the bearing capacity of strip footing. The relationship obtained between footing aspect ratio and shape factor from the finite element results can express through simple quadratic equations. The equations gives comparatively higher shape factor for slender footing and reduced shape function for square and rectangular footing for lower aspect ratio.

Kinematic Failure Mechanisms of Rough Footing Interface

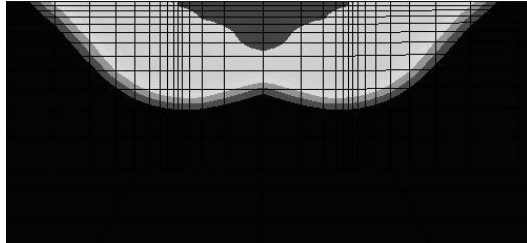
Figure 4 represents the contours of resultant soil displacement at failure for each of the footings modeled. As the footings becomes larger the wedge underneath the footing becomes deeper and additional sliding wedge developed. At the same time the central wedge is getting sharper and smaller.



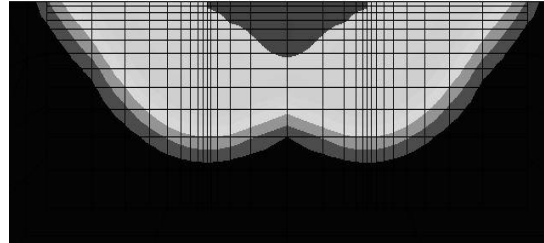
(a) $L/B=1$



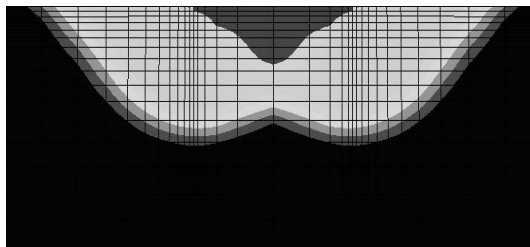
(b) $L/B=2$



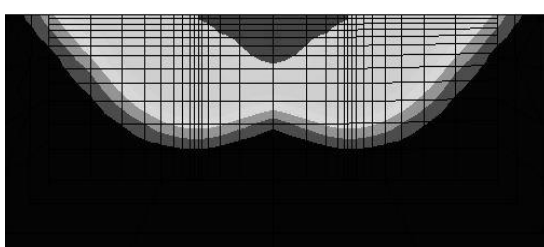
(c) $L/B=3$



(d) $L/B=4$



(e) $L/B=5$

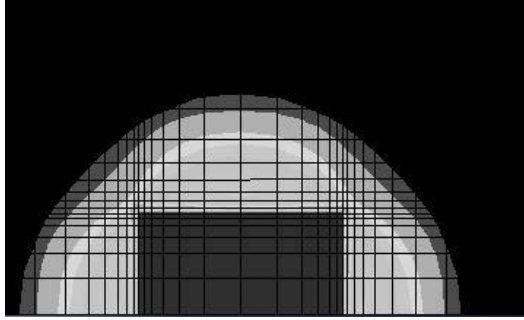


(f) $L/B=8$

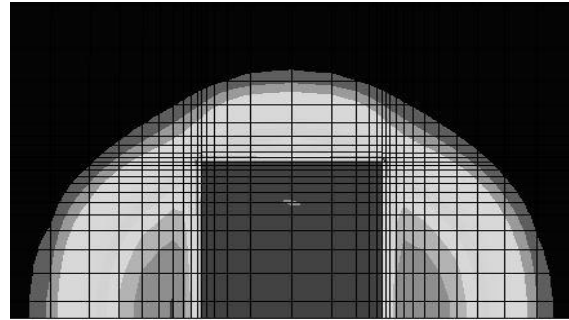
Figure 4: Kinematic failure mechanisms of footings of various aspect ratio (rough interface)

(a) $L/B=1$; (b) $L/B=2$; (c) $L/B=3$; (d) $L/B=4$; (e) $L/B=5$; and (f) $L/B=8$.

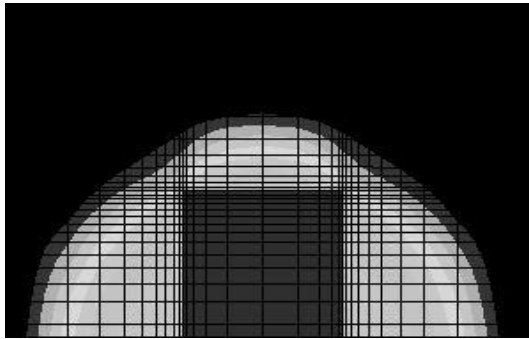
Consideration of the regions of displaced soil, viewed in plan as illustrated in Figure.5 (a–f), shows the failure mechanism extender in the longitudinal direction i.e., along the long axis is independent of footing aspect ratio, and equal to approximately $0.6B$. Diagonal symmetry for the square footing of the failure mechanism is also clearly illustrated by the displacement contours shown in Figure.5. It could also be surmised from the displacement contours in Figure.6 that plane strain conditions prevail approximately $1.5B$ from the end of the footing, measured along the long axis.



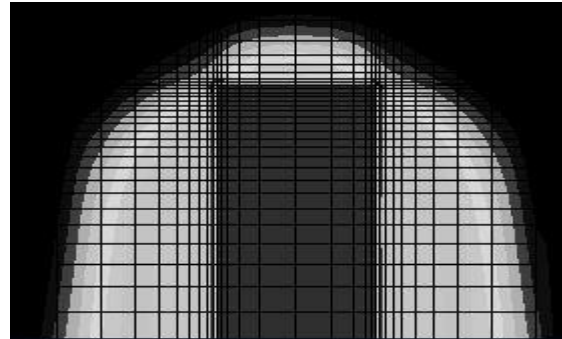
(a) $L/B=1$



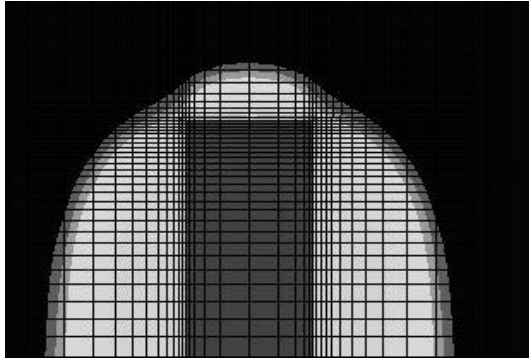
(b) $L/B=2$



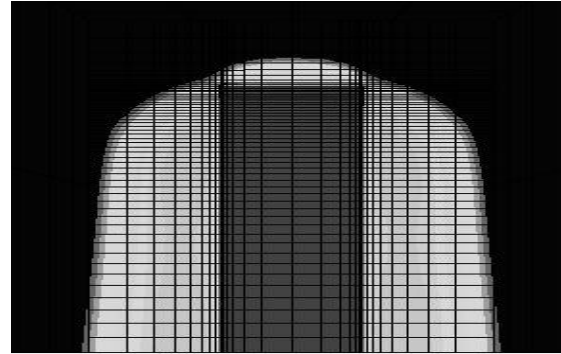
(c) $L/B=3$



(d) $L/B=4$



(e) $L/B=5$



(f) $L/B=8$

Figure 5: Plan view of failure mechanisms (rough footings) (a) $L/B=1$; (b) $L/B=2$; (c) $L/B=3$; (d) $L/B=4$; (e) $L/B=5$; and (f) $L/B=8$.

Smooth footing Interface

The kinematic mechanism of failure observed in the finite element analysis for the smooth square footing indicating double wedge hill type mechanism where no central edge is evident in the Figure 7 and the slip taking place underneath footing moving towards the outer edge at an angle α (Figure 6). Some soil movement occurred directly below the center of the footing.

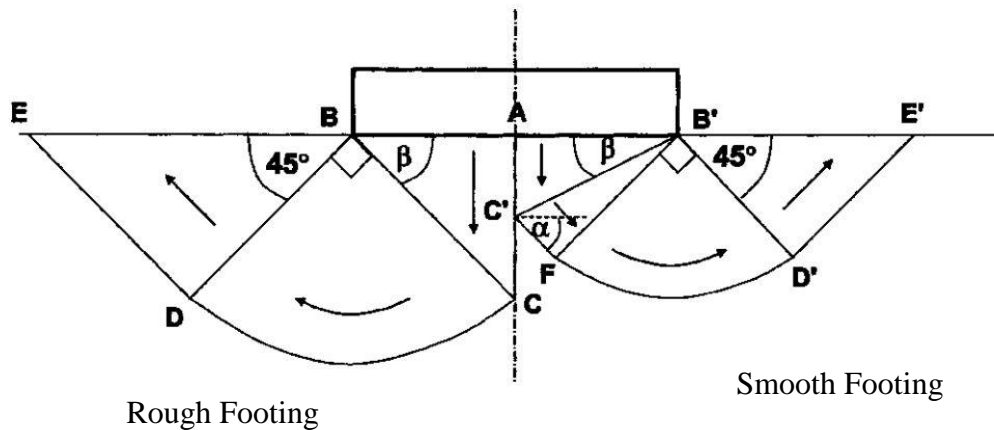


Figure 6: Typical kinematic failure mechanism of rough and square footing

The failure depth or influence zone of rough square footing is much higher than smooth square footing. It represents that the bearing capacity of rough square footing is higher than the smooth square footing. The central edge is clearly visible for rough square footing which is absent in smooth square footing. As the uniform vertical load applied at the rough footing only one direction so central edge developed but for smooth square footing the displacement freed to all directions so no central edge developed.

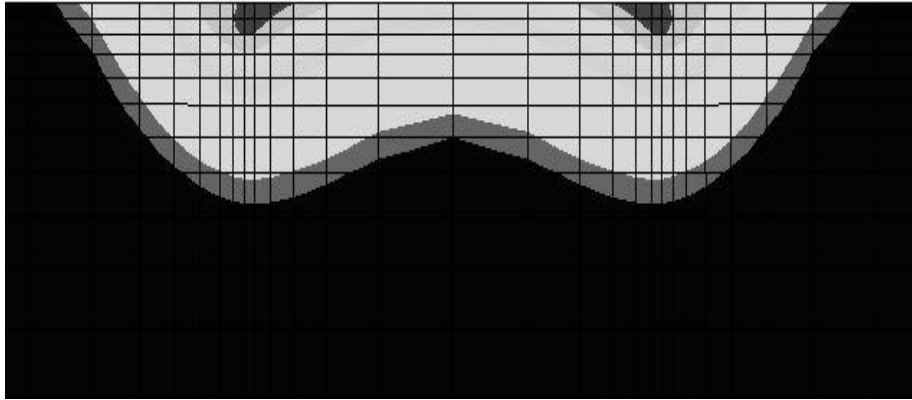
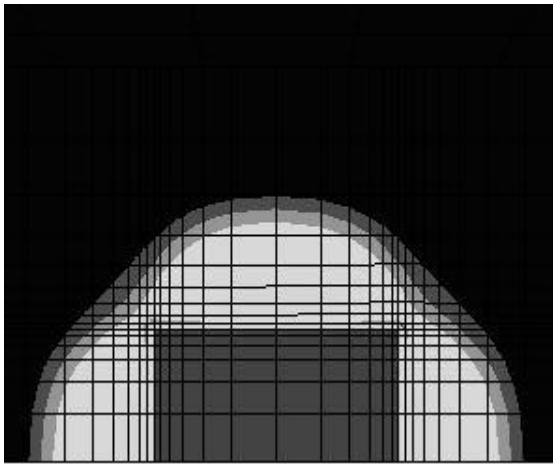
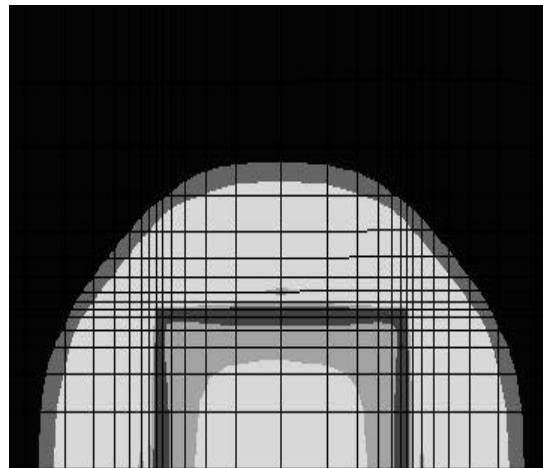


Figure 7: Kinematic Failure mechanism of smooth square footing

Contours of resultant displacement viewed in plan over through and smooth square footings are shown in Figure 8. These also illustrate the variation in nature of the soil displacement depending on interface roughness. The footings are subjected to a uniform vertical displacement; the contours of resultant displacement beneath the rough footing show that the soil moves uniformly vertically downwards with no relative soil movement on the underside of the footing. The contours beneath the smooth footing show a variation of soil displacement across the footing area, the maximum soil movement occurring at the footing periphery with less displacement beneath the center.



(a) Rough



(b) Smooth

Figure 8: Displacement contours at failure for square footings (a) rough; (b) smooth.

3.2 Equations

The best estimate equation between shape factor and footing aspect ratio for rough rectangular footings is shown on equation (1) and for smooth rectangular footing is shown on equation (2).

$$S_c = 0.999 + 0.1896(B/L) - 0.0502\left(\frac{B}{L}\right)^2 \quad (1)$$

Where, $R^2=1$, S_c = Shape factor of footing, B/L = Aspect ratio

And for smooth rectangular footing is,

$$S_c = 1.009 + 0.1035(B/L) - 0.0323\left(\frac{B}{L}\right)^2 \quad (2)$$

Where, $R^2=0.99$, S_c =Shape factor.

3.3 Tables

Comparison of Undrained Bearing Capacity and Shape Factors results of the finite element analyses is shown on Table 1 with the results obtained by Skempton (1951) and Salgado et al.

Table 1: Comparison of Undrained Bearing Capacity and Shape Factors for Smooth and Rough Based Rectangular Footings

L/B	Rough Footing		Smooth Footing		Skempton(1951)		Salgado et al.		
	<i>N_c</i>	<i>S_c</i>	<i>N_c</i>	<i>S_c</i>	<i>N_c</i>	<i>S_c</i>	<i>LB</i>	<i>UB</i>	<i>Avg</i>
1	5.99	1.14	5.64	1.07	6.17	1.20	5.52	6.22	5.87
2	5.69	1.08	5.48	1.04	5.65	1.10	5.36	6.02	5.69
3	5.56	1.06	5.42	1.03	5.48	1.07	5.25	5.89	5.57
4	5.49	1.04	5.39	1.03	5.39	1.05	5.2	5.85	5.525
5	5.44	1.04	5.37	1.02	5.35	1.04	5.17	5.78	5.475
8	5.37	1.02	5.33	1.01	5.25	1.02	5.15	5.57	5.36

4. CONCLUSIONS

- Bearing capacity of rough square footing is 5.36% greater than smooth square footing and rough based rectangular footing has larger bearing capacity factor and shape factor with greater aspect ratio. Bearing capacity of smooth footing is 3.66% lower than rough rectangular footing.
- The best fit equation from the relationship between shape factor and aspect ratio for rough and smooth rectangular footing is derived.
- The difference of bearing capacity between rough and smooth square and rectangular footing decreases with the decrease of footing aspect ratio. The more the footing strip the minimum the difference of bearing capacity and shape factor.

ACKNOWLEDGEMENTS

I would like to thank assistant professor Md. Shafiqul Islam who inspired and helped me in the whole works and professor Md. Rokonzaman who guided me as a supervisor completing the works properly.

REFERENCES

- Cox, A. D., Eason, G., and Hopkins, H. G. 1961. "Axially symmetric plastic deformation in soils." *Proc. R. Soc. London, Ser. A*, 254, 1–45
- De Beer, E. E. 1970. "Experimental determination of the shape factor and the bearing capacity factors for sand." *Geotechnique*, 204, 387–411. *Geotechnique*, 519, 787–798.

- Hansen, B. J. 1970. "A revised and extended formula for bearing capacity." *Bulletin 28*, Danish Geotechnical Institute Copenhagen, Denmark.
- Levin, E. 1955. "Indentation pressure of a smooth circular punch." *Q. Appl. Math.*, 132, 133–137.
- Michalowski, R. L., and Dawson, E. M. 2002. "Three-dimensional analysis of limit loads on Mohr–Coulomb soil." *Foundations of civil and environmental engineering*, Vol. 1, Poznan University of Technology Press, Poland,
- Michalowski, R. L. 2001. "Upper bound load estimates on square and rectangular footings."
- Salgado, R., Lyamin, A. V., Sloan, S. W., and Yu, H. S. 2004. "Two and three-dimensional bearing capacity of foundation in clay." *Geotechnique*, 545, 297–306.
- Shield, R. T., and Drucker, D. C. 1953. "The application of limit analysis to punch indentation problems." *J. Appl. Mech.*, 20, 453–460.
- Skempton, A. W. 1951. "The bearing capacity of clays." *Proc., Building and Research Congress*, Vol. 1, London, 180–189.
- Shield, R. T., and Drucker, D. C. 1953. "The application of limit analysis to punch indentation problems." *J. Appl. Mech.*, 20, 453–460
- Skempton, A. W. 1951. "The bearing capacity of clays." *Proc., Building and Research Congress*, Vol. 1, London, 180–189.
- Terzaghi, K. 1943. *Theoretical soil mechanics*, Wiley, New York. 37–147.